The 8th International Conference on Jets, Wakes andSeparated Flows, ICJWSF-2024
September 23-25, 2024, Firenze, Italy

Loss reduction in the flow through an elbow tube with sharp-edged corner by using a weir-shaped obstacle

Toshitake ANDO[1*], Hayato Kane[1], Kenta Ono[1], Shohei Aoki[1], Koichi Tsujimoto[1] and Mamoru Takahashi[1]

1: Graduate School of Engineering, Mie Univ., Japan

* Corresponding author: ando@mach.mie-u.ac.jp

Abstract

In this study, loss reduction for circular elbow pipe by simple method with weir-shaped small obstacle is presented. Ordinary ways to reduce the loss of elbow pipes are chamfering or rounding its inner corner and/or mounting guide vanes near the corner. The method proposed in this study is simpler than these methods and is considered that it is easier to retrofit to elbows with corners. The pressure distribution along pipe axes and pressure loss were measured while changing the distance between the small obstacle and the inner corner of the elbow and the obstacle height in order to find the conditions of obstacle which make the loss become smallest, and then the effects of the obstacle on the separated flow were clarified by numerical calculation.

Keyword:*Circular elbow pipe, Separation control, Flow resistance, Loss reduction*

1. Introduction

Elbow and bend are the kind of pipe elements which change the direction of pipe arrangement, and are used in order to place long pipes in a small space and to passing pipes through narrow, intricate spaces between equipments. The fluid passing through this kind of pipe elements is unable to follow the pipe curvature because of its own inertia, is separated from inner corner of the elbow and flows away from the wall including the corner. The decreased effective cross-sectional area due to flow separation causes large pressure loss occurs in this type of pipe element [4]. The pressure loss increases the power to transfer the fluid. In order to reduce additional power due to this type of pressure loss, some control of separated flow from the corner of elbow is needed. The purpose of this study is to reduce the loss by simpler way.

Ordinary ways to reduce the loss of elbow pipes are chamfering or rounding its inner corner and/or setting guide vanes near the corner [4]. These ways require machining corner edge in the case that it is originally sharp or setting relatively large equipments on the pipe wall, therefore they are difficult to retrofit to pipe systems.

On the other hands, some simpler way which uses half trip [6] or weir-shaped obstacle was proposed. This method aims to reduce losses by making separated flow from the corner of obstacle to have a direction of the downstream pipe/duct wall. This is easier to retrofit to elbows with sharp-edged inner corner than rounding or chamfering corner, and uses simpler object than guide vanes. For examples of applications to pipe/duct system similar to elbow pipes, there are counter type flow confruent in T-junction especially the case of the 1:0 ratio of confruent flow rate[1, 3] and flow through reducing elbow of square duct especially the case of contraction ratio of 1:0[2]. In the case of T-junction pipes and reducing elbow ducts, the mean flow velocity in the upstream of them is slower than the downstream of them so that loss of obstacle in the upstream is relatively small, whereas the flow downstream, where the mean flow velocity is high and the penalty for the reduction in effective cross-sectional area is large, is controlled. This allows the installation of a relatively tall obstacle to reduce losses. Afterwards, it was found that losses could be reduced by short obstacle even in T-junction pipes with confluent ratio of 1:0 and in normal elbow ducts without section reducing.

In this study, mounting weir-shaped obstacle is applied to circular elbow pipe of 90° with sharp-edged corner, and the effects of the obstacle on pressure distribution and loss were investigated by changing the distance between the small obstacle and the inner corner of the elbow and the obstacle height.

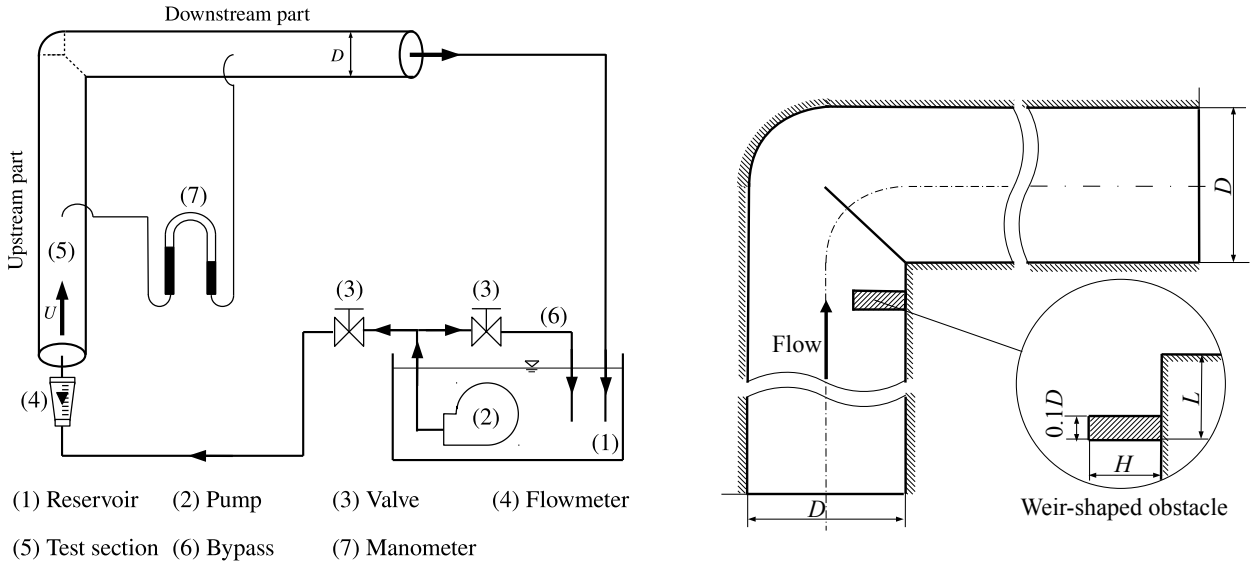

(a) overall view of the setup

(b) details around the elbow part

Fig. 1: Experimental Setup

2. Experimental Setup and Procedure

Figure 1 (a) shows the outline of experimental setup. In this study, the working fluid is tap water and the water stored in the reservoir tank (1) was driven by a pump (2), and after branching off from the bypass (6) and passing through the flow control balve (3) and flowmeter (4), it was led to the test section (5) placed horizontally. The water passed through the test section and the bypass was returned to the reservoir tank. The test section has $D = 0.030$ [m] of inner diameter, and two straight regions of $70D$ length upstream and downstream of elbow part. These straight parts are acrylic extruded round tubes. There were multiple pressure taps along the pipe axis at the apex of the cross sections of the test section, and the pressure distribution was measured by an inverted U tube manometer (7) connected to those pressure taps.

A details of elbow part is shown in Fig. 1 (b). The elbow section consists of two concave cylindrical surfaces and a quarter concave spherical surface. In another words, outer corner of miter elbow was rounded by the concave sphere having radius of the pipes those concave cylindrical surfaces make line of intersection of a half circle and at they make sharp edge at the half circle. The x- and y-axis are parallel to the central axis of the upstream and downstream parts and in the same direction as the main flow, respectively, and the origin is located at the inlet of the elbow part.

Experiments in which pressure distributions and pressure loss are measured by using tap water at the Reynolds number Re ($= UD/\nu$, U: mean verocity, D: inner diameter of the pipe, ν kinematic viscosity) of 3.0×10^4 were conducted. The obstacle height H and the distance between the front surface of the obstacle and elbow corner L were changed in the region of $0.15 \leq H/D \leq 0.25$ and $0.2 \leq L/D \leq 0.7$ to find the combination (H, L) in which makes pressure loss minimum.

Figure 2 shows a schematic diagram of pressure distribution parallel to the central axis of the pipe. The horizontal axis represents the dimensionless position s/D ($s/D = 0$ corresponds to the inlet of the elbow), and the vertical axis represents the pressure coefficient. There are fully developed regions in the upstream and downstream parts. Extending each linear pressure distribution to the origin, the pressure difference between the upstream and downstream parts at $s/D = 0$ is found. Or extending the pressure distribution in the fully developed region on the upstream side to the downstream part, the difference between the extrapolated pressures and the actual pressure in the downstream part is found. The pressure loss was calculated from latter pressure difference in this study.

In the experiment, the tap of reference pressure was located on the upstream part, so that it was confirmed that the pressure in the fully developed region on the upstream part remained almost unchanged regardless of the object conditions by limited measurements. Therefore the entire pressure distribution on the upstream side was measured only in the case without object. In the cases with obstacle, pressure distribution only in

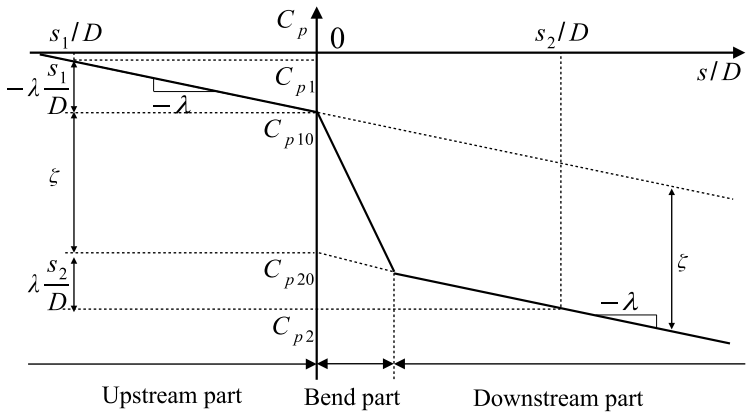

Fig. 2: Definition of the pressure loss coefficient ζ

Tab. 1: Conserved quantity, diffusivity and source

	ϕ^*	Γ	S^*
mass	1	0	0
momentum	$\boldsymbol{V}^*$	$\frac{1}{\mathrm{Re}}+\nu_t^*$	$-\boldsymbol{\nabla}^* p^*$
turbulent energy	k^*	$\frac{1}{\mathrm{Re}}+\frac{\nu_t^*}{\sigma_k}$	$G^*-\varepsilon^*$
disspation rate of k	ε^*	$\frac{1}{\mathrm{Re}}+\frac{\nu_t^*}{\sigma_\varepsilon}$	$C_1 G^*\frac{\varepsilon^*}{k^*}-C_2\frac{\varepsilon^{*2}}{k^*}$

$\nu_t^*=C_\mu\frac{k^{*2}}{\varepsilon^*}$, $G^*=\frac{\partial u_i^*}{\partial x_j^*}\left(\frac{\partial u_i^*}{\partial x_j^*}+\frac{\partial u_j^*}{\partial x_i^*}\right)$ $(i=1,2,3)$

$C_\mu=0.09$, $\sigma_k=1.0$, $\sigma_\varepsilon=1.3$, $C_1=1.44$, $C_1=1.91$

the fully developed region on downstream part except in the case of maximal loss reduction.

3. Numerical Methods

To investigate the effect of a obstacle on the characteristics of the flow field, numerical simulations for the mean flow without obstacle and with a obstacle which was found that the pressure loss was reduced most by experiments. The governing equations are the Reynolds averaged continuity equation (SIMPLE method[7]) and Navier-Stokes equations with turbulent viscosity, and additionally the transport equations for the turbulent kinetic energy k and its dissipation rate ε (standard k-ε turbulence model [5]). These equations are expressed as following form:

$$\boldsymbol{\nabla}\cdot(\boldsymbol{V}^*\phi^*)=\boldsymbol{\nabla}^*\cdot(\Gamma^*\boldsymbol{\nabla}\phi^*)+S^*$$

where, $*$ means nondimensional value and ϕ^*, Γ^* and S^* are given in Tab. 1. OpenFOAM was used as the solver.

Uniform velocity parallel to pipe wall, zero pressure gradient and k and ε based on turbulence intensity of 5% were given as the inlet boundary conditions. Zero gradient of velocity and turbulence amounts, and zero pressure were given as the outlet boundary conditions. Wall function based on a logarithmic low and zero pressure gradient were given on the pipe wall.

Numerical simulations with the same Reynolds number as in the experiment were carried out in two cases: the case without obstacle and with obstacle of condition which pressure loss was minimized in the experiment. The effects of the obstacle on the flow characteristics around the elbow were investigated.

4. Results and Discussion

4.1. Effects of obstacle on pressure distribution

Figures 3 (a) and (b) show the effect of the obstacle height H/D and the mount position L/D of the obstacle on the pressure distribution, respectively. The axes of these figures are the same as in Fig. 2, and

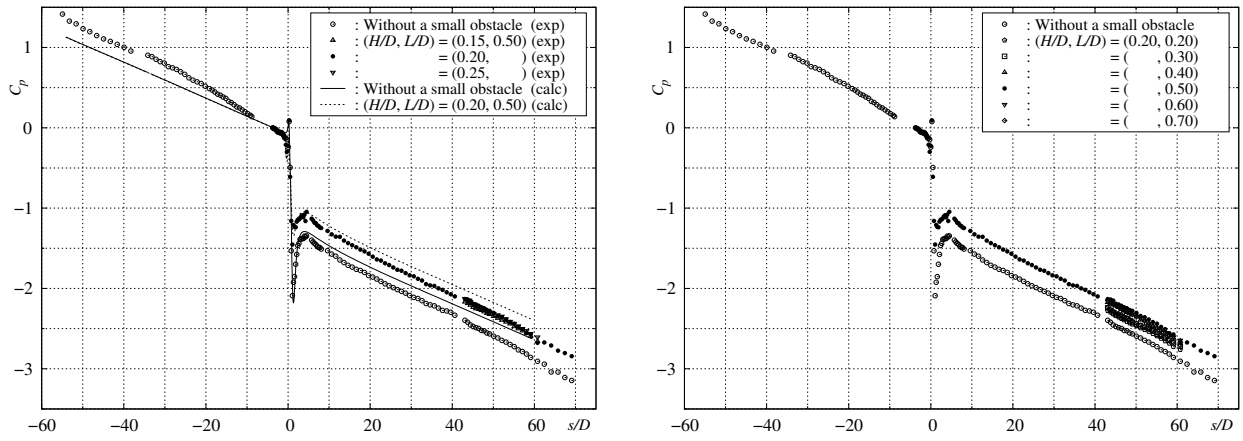

(a) effects of H/D (b) effects of L/D (exp)

Fig. 3: Effects of obstacle on pressure distribution

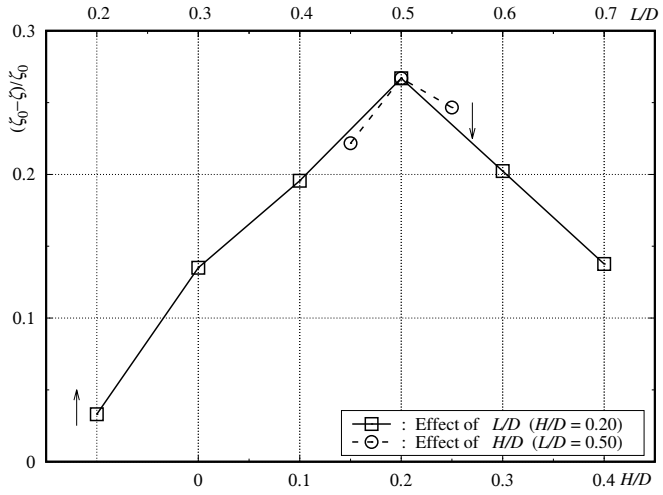

Fig. 4: Effects of obstacle on pressure loss coefficient (exp)

the results for the cases without the obstacle and with the obstacle of $(H/D, L/D) = (0.2, 0.5)$ are included in both figures. The pressure in the upstream part decreased at a constant gradient from the inlet to the elbow. After the flow enter the elbow part, the pressure increased once, reaching a maximum of about 0.08 at $s/D = 0.26$, then it suddenly decreased and reached a minimum of -2.09 at $s/D = 1.05$. Then the pressure recovered, reaching a maximum of -1.35 at $s/D = 4.52$, before gradually decreasing with a constant gradient.

On the other hand, in the case of small obstacle of $(H/D, L/D) = (0.2, 0.5)$, the change in pressure around the elbow was smaller than the case without small objects with the minimum and second maximum values being -1.45 and -1.05, respectively. The change from minimum to maximum became the half that in the case without obstacle. As a result, in the cases with obstacle, the pressure in the fully developed region in the downstream part becomes higher than the case without the obstacle, and the loss coefficient ζ decreased from 1.06 without obstacle to a minimum of 0.77 by mounting the obstacle.

The solid and dashed lines in the Fig. 3 (a) show the results of the numerical simulation in the cases without obstacle and with obstacle of $(H/D, L/D) = (0.2, 0.5)$, respectively. The pressure gradients in the fully developed regions in the upstream and downstream parts are different between the experiment and the simulation. Both are different from the gradients due to the pipe friction loss of the circular pipe from the Blasius equation. It is thought that the experimental ones differ from the value obtained from the equation due to the tolerance of the inner diameter of extruded acrylic pipe. However, the numerical simulation results agree with the experimental ones for the change in pressure from the inlet of elbow part to the appearance of the second maximum value. Regarding the pressure loss ζ, it is 1.211 and 0.969 without obstacle and with

obstacle of $(H/D, L/D) = (0.2, 0.5)$, respectively, which differ from the experimental results by 14–26%, but qualitatively shows the reduction in loss due to mounting of obstacle.

4.2. Effects of obstacle on the loss

Figure 4 shows the effects of obstacle height H/D and obstacle position L/D on the reduction ratio of pressure loss factors. This figure has a vertical axis and two horizontal axes. The vertical axis represents the reduction rate ζ, $(\zeta - \zeta_0)/\zeta_0$ (ζ_0: ζ in the case without obstacle). The upper horizontal axis and lower one represent L/D and H/D, respectively.

The the loss ζ in all cases shown in this figure was reduced by using obstacle. The reduction rate of the loss takes maximum value for both of L/D, H/D, and the condition which the loss is reduced the most is $(H/D, L/D) = (0.2, 0.5)$.

The pressure in the low pressure region downstream near the corner increased with the mounting of the object, and then the pressure in the downstream fully developed region also increased. It is seemed that effective cross-sectional area of the flow near the corner was enlarged by reduction of vortex region on the wall downstream of the corner and loss reduction due to shrinking of the vortex region larger than the increase in loss caused by the mounting obstacle.

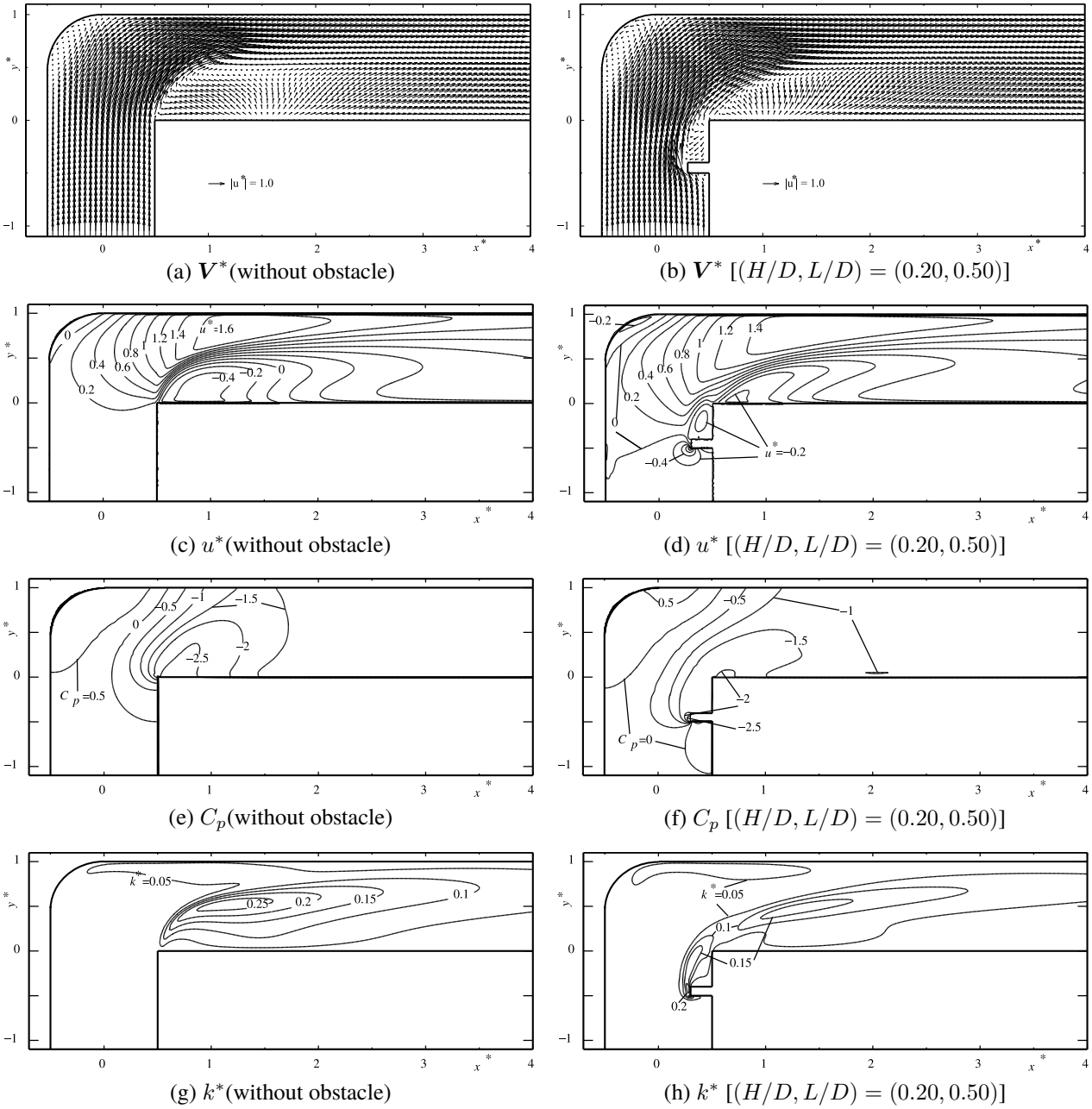

(a) $\boldsymbol{V}^*$(without obstacle) (b) $\boldsymbol{V}^*$ $[(H/D, L/D) = (0.20, 0.50)]$

(c) u^*(without obstacle) (d) u^* $[(H/D, L/D) = (0.20, 0.50)]$

(e) C_p(without obstacle) (f) C_p $[(H/D, L/D) = (0.20, 0.50)]$

(g) k^*(without obstacle) (h) k^* $[(H/D, L/D) = (0.20, 0.50)]$

Fig. 5: Effects of obstacle on the flow (calc; $z^* = 0$)

4.3. Effects of obstacle on flow characteristics

Figure 5 shows the effect of the obstacle on the velocity vector field and the distribution of various quantities obtained by numerical simulation. In this figure (a) and (b) show the velocity vector field, (c) and (d), (e) and (f), and (g) and (h) show the distribution of the velocity component in x-direction, u^*, the pressure coefficient, C_p, and the turbulent kinetic energy, k^*, respectively. Additionally, (a), (c), (e) and (g) show the results without obstacle, and (b), (d), (f) and (h) show the case of $(H/D, L/D) = (0.2, 0.5)$.

In the case without obstacle, the flow separated from the elbow corner at an angle of about 80° to the x-axis and flowed about 0.7 away from the inner wall [Fig. (a)]. As a result, u^* in the region from $x^* = 1$ to 2 outside the separated streamline increased to about 1.6 [Fig. (c)], and the pressure near the inner wall takes the value in the range from -2.5 to -2 [Fig. (e)].

On the other hand, in the case of $(H/D, L/D) = (0.2, 0.5)$, the angle of flow at the elbow corner is reduced to about 40°, and the separated streamline passes near the pipe center, and the distance between it and the inner wall is reduced [Fig. (b)]. The maximum velocity outside the separated streamline is reduced to 1.4 [Fig. (d)], and the pressure near the inner wall downstream of the corner changes to the range of -1.5 to -2.0 [Fig. (f)]. This corresponds to the change in pressure distribution along the pipe axis and the reduction in loss due to the mounting the obstacle.

It is seemed that the because of slowing down the change in velocity at the downstream inlet by mounting obstacle the maximum value of the turbulent kinetic energy in this section also changed from 0.25 to 0.15 [Fig. (g), (h)].

5. Conclusion

Main results are summarized as follows:

1. Most cases with an obstacle which we examined made a pressure loss ζ smaller than the case without obstacle. In the case of $(H/D, L/D) = (0.2, 0.5)$, ζ was reduced maximum 26%.
2. The condition of minimum pressure loss $(H/D, L/D) = (0.2, 0.5)$ was similar to the case of counter type flow confruent in the T-junction of the 1:0 ratio of confruent flow rate $(H/D, L/D) = (0.2, 0.47)$ [1, 3] and the case of the flow through the elbow of square duct $(H/D, L/D) = (0.2, 0.65)$ [2].
3. Numerical simulation results using the standard k-ε turbulence model qualitatively shows the reduction of loss of the flow through elbow by mounting of an obstacle. The results show that the mounting of obstacle reduces the angle of the flow passing through the elbow corner and the separated flow flows close to the inner wall.

References

[1] Toshitake ANDO et al. “Drag Reduction of T-junction Pipe Flow by Small Obstacles”. In: *Journal of Fluid Science and Technology* 6.4 (2011), pp. 614–624. DOI: 10.1299/jfst.6.614.

[2] Toshitake ANDO et al. “Effects of contraction ratio on loss reduction of the flow in the reducing elbow duct with a weir-shaped obstacle”. In: *Journal of Fluid Science and Technology* 18.1 (2023), JFST0010–JFST0010. DOI: 10.1299/jfst.2023jfst0010.

[3] Toshitake ANDO et al. “Effects of flow rate ratio on loss reduction of T-junction pipe”. In: *Journal of Fluid Science and Technology* 9.3 (2014), JFST0045–JFST0045. DOI: 10.1299/jfst.2014jfst0045.

[4] Hideki Hibara et al. “Rectifying Effects of Guide Vanes on the Flow Downstream from the Bend”. In: *Turbomachinery* 29.8 (2001), pp. 472–481. DOI: 10.11458/tsj1973.29.472.

[5] B. E. Launder and D. B. Spalding. “The numerical computation of turbulent flows”. In: *Computer Methods in Applied Mechanics and Engineering* 3.2 (1974), pp. 269–289. ISSN: 0045-7825. DOI: 10.1016/0045-7825(74)90029-2.

[6] Shinsuke MOCHIZUKI et al. “Drag Reduction in a 90-degree Bend Pipe with a Half-Trip”. In: *Transactions of the Japan Society of Mechanical Engineers Series B* 69.679 (2003), pp. 595–601. DOI: 10.1299/kikaib.69.595.

[7] S. V. Patankar and D. B. Spalding. “A calculation procedure for heat, mass and momentum transfer in three-dimensional parabolic flows”. In: *International Journal of Heat and Mass Transfer* 15.10 (1972), pp. 1787–1806. ISSN: 0017-9310. DOI: 10.1016/0017-9310(72)90054-3.